

2008

# Impact of Power Frequency on the Performance of a Scroll Compressor

Michael M. Cui

*Trane*

Jack Sauls

*Trane*

Follow this and additional works at: <https://docs.lib.purdue.edu/icec>

---

Cui, Michael M. and Sauls, Jack, "Impact of Power Frequency on the Performance of a Scroll Compressor" (2008). *International Compressor Engineering Conference*. Paper 1903.

<https://docs.lib.purdue.edu/icec/1903>

This document has been made available through Purdue e-Pubs, a service of the Purdue University Libraries. Please contact [epubs@purdue.edu](mailto:epubs@purdue.edu) for additional information.

Complete proceedings may be acquired in print and on CD-ROM directly from the Ray W. Herrick Laboratories at <https://engineering.purdue.edu/Herrick/Events/orderlit.html>

## Impact of Power Frequency on the Performance of a Scroll Compressor

Michael Cui<sup>1\*</sup> and Jack Sauls<sup>2</sup>

<sup>1</sup>TRANE  
La Crosse, WI 54601 USA  
608-787-3313  
mcui@trane.com

<sup>2</sup> TRANE  
La Crosse, WI 54601 USA  
608-787-2517  
jsauls@trane.com

### ABSTRACT

The impact of the power frequency on the performance of a scroll compressor was investigated. Two representative frequencies, 50 and 60 Hz, were used to quantify the effects of the power frequency on the scroll compressor performance characteristics for the same design. The major physical mechanisms responsible for the scroll compressor performance were identified. The changes induced by the power frequency on these physical mechanisms were illustrated by numeric simulations and laboratory measurements of the detailed flow physics inside the scroll compressor. The design parameters were obtained by integrating the field quantities over the relevant regions. The link between the design features and flow physics was established. The new design ideals can be generated from the fundamental understanding the physical mechanisms induced by the power frequency change.

### 1. INTRODUCTION

A scroll compressor typically is required to perform well for the electric power with 50 and 60 Hz frequencies. This requirement is the result of the globalization of the compressor industry since the 50 and 60 Hz are the most common power frequencies available for compressor users over the world. The scroll compressors also sometimes are driven by variable frequency drives to optimize the part-load performance. When the scroll compressors operate on these conditions, different characteristics of the flow physics are observed inside the scroll compressors. The fundamental changes in the flow field lead to different performance levels for the same compressor design.

The power frequency change also causes variations of mechanical loss and motor efficiency. Park *et al.* (2002) developed a correlation between frequency and mechanical loss using the data obtained by Cho *et al.* (1996) and Hirano *et al.* (1988). They also introduced a motor performance curve as a function of frequency using the test data.

This paper documents a study on the physical phenomena inside the compressor flow field associated with the power frequency. The study is focused at the performance level and losses associated with fluid mechanics and heat transfer inside the scroll compressor. A refrigeration scroll compressor is chosen for this project. The design specifications of the compressor are as follows:

Power frequency, Hz	Rotating speed, rpm	Pressure ratio	Inlet pressure, kN/m <sup>2</sup>	Inlet temperature, °C	Discharge temperature, °C
60	3500	3.90	372	18	81
50	2920	3.90	372	18	81

**Table 1** Compressor operating conditions at design point.

Both static and dynamic features of the compressor are included in the analysis. Refrigerant R134a is used as the working fluid. The power sources with output frequencies of 50 and 60 Hz are used for the same scroll compressor. Two cases are investigated comparatively. The changes induced by the power frequencies are analyzed by the differences between the two cases. The detailed changes on the suction, compression, and discharge processes are simulated numerically. The loss mechanisms in these processes are analyzed in detail. The overall performance of the scroll compressor is calculated from the detailed flow physics to quantify the impact of the power frequency on the compressor. The results obtained are validated by laboratory measurements of the static and dynamic quantities. The relationship between the design details and loss mechanisms are defined. The methodology and the data obtained can be applied to design and optimization of the scroll compressors that will perform well with both 50 and 60 Hz electric power.

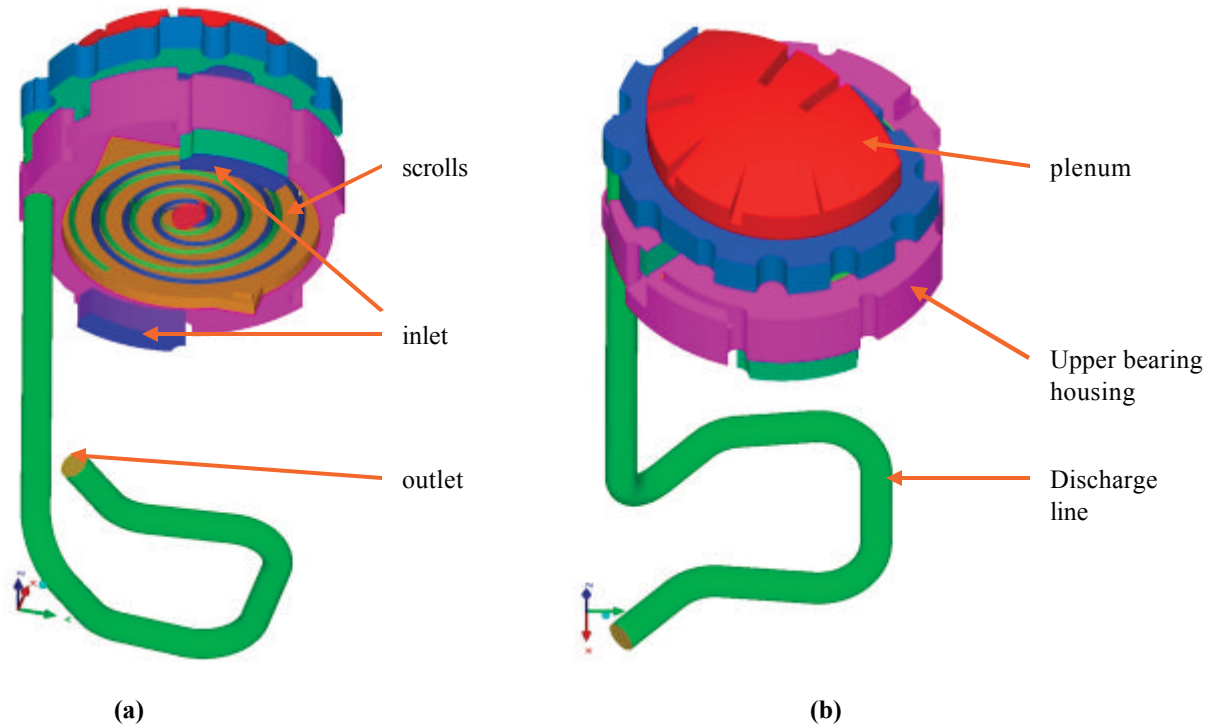


**Figure 1 Scroll compressor model: bottom view (a) and top view (b).**

A complete scroll compressor working process can be divided into three parts: suction, compression and discharge. The continuative gas flow stream is separated into a series of individual gas pockets with crescent shapes during the suction process. The gas pockets are compressed when they move from the circumference of the scroll compressor to its center. These individual gas pockets merge together during the discharge process. A continual gas stream with higher pressure and temperature is formed by merging the individual gas pockets at the discharge port and eventually leaves the compressor. When the power frequency changes, it affects three processes differently. For a given design, the geometric features of the compressor are the same for the different power frequencies. The changes only happen on the dynamic features. The sizes and shapes of the gas pockets are the same for the different frequencies. Consequently, the pressure ratio is kept the same. However, the speed of the opening, closing, and merging processes depends on the orbiting frequency of the scroll. The time needed for suction, compression and discharge processes are longer for lower frequency. The time interval for the gas pockets moving from the inlet to the discharge port is longer as well. Consequently, the refrigerant gas leaks from high pressure gas pockets to low pressure gas pockets. The leakage loss is larger at lower frequency. When gas pockets reach the center of the compressor, they start to merge with each other from the two sides of the compressor. The individual gas pockets become a continuative stream again. When the power frequency increases, the merging, mixing, and diffusion associated with discharge process are intensified. The losses associated with discharge process are larger. All these physical mechanisms and their interactions are investigated in an integrated fashion. The definition of the changes induced by the power frequency variation in these mechanisms provides a foundation to optimize compressor design. To achieve this objective, each of the aforementioned mechanisms is quantified separately and studied

comparatively for the 50 and 60 Hz cases. The working fluid is Refrigerant R134a. The geometric features of the compressor are illustrated in Figure 1. The details of the numerical model and data processing techniques have been described by Cui (2003) and Cui and Sauls (2006).

## 2. SUCTION PROCESS

The suction process starts when the refrigerant gas enters the upper bearing housing (Figure 1). The gas from the inlet, two openings on the upper bearing housing, fills the space around the scrolls. When the suction chambers open, the pressure differential between the space inside the suction chambers and surrounding regions drives the refrigerant gas into two suction chambers. The through-flow areas of the two suction chambers as a function of time are illustrated in Figure 2 (a). The volumes of two suction chambers as functions of time are shown in Figure 2 (b). The rate of the volume expansion of the suction chambers depends on the power frequency of the scroll compressor (Figure 2). The through-flow area of the 60 Hz case opens and closes at a rate of 20% quicker than the 50 Hz case. The corresponding volume for 60 Hz case also reaches its maximum value 20% faster than the 50 Hz case. Since the profiles of the involutes for the fixed and orbiting scrolls are essentially same, the suction chambers on the two sides of the scroll compressor show identical profiles of the area and volume variations.

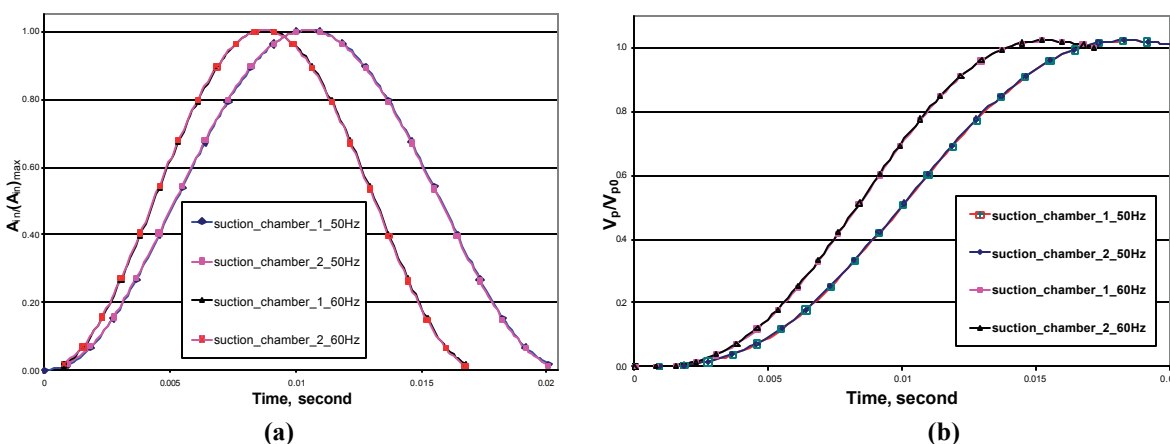


**Figure 2 Flow area (a) and volume (b) of the suction chambers for the frequency of 50 Hz and 60 Hz.**

The physical quantities show much more complex phenomena than the geometric features for power frequency change. Figure 3 and Figure 4 show the pressure and temperature histories inside the suction chambers. The pressure and temperature inside the suction chambers start from the higher value and decrease rapidly to reach its bottom. The recovery processes from the minimum values are monotonic and the pressure and temperature eventually exceed their starting values of the suction process. Compared to the pressure profiles, the temperature profiles show a slower response to the orbiting motion of the suction process (Figure 4). The temperature change depends on multiple factors: the volume change of the suction chambers, the boundary friction, and kinetic dissipation. The boundary friction and dissipation of the kinetic energy occurs later since they are induced by the pressure drawdown. The temperature changes are modulated by these two factors and show different profiles from the pressure.

Different from their geometric features, the asymmetry of pressure and temperature distributions inside the two suction chambers exists in both the 50 and 60 Hz cases. The pressure and temperature on the two opposite sides of the compressor show very different profiles. Suction chamber 1 shows a faster pressure drawdown at the beginning of the suction process. Since the asymmetric features of the two sides are not observed in the geometric features, the differences between the two sides are induced by the dynamic nature of the process. This explains that the degree of the asymmetry of the pressure and temperature profiles of the suction chambers located on the two sides of the compressor in the 60 Hz cases is stronger than the 50 Hz cases. Although the shapes and sizes of the suction chambers are the same on the two sides, the moving boundaries of the gas pockets are different. Figure 5 and Figure 6 show the velocity entering the suction chambers for the 50 and 60 Hz cases. Asymmetry of the velocity profiles can be observed in both 50 Hz and 60 Hz cases. The velocity is generated by the moving walls and pressure difference between the gas pockets and surrounding space. As the results, the profiles of the velocity distributions

are different from the pressure distributions. However, the asymmetric features in the velocity distributions can be observed in Figure 5 and Figure 6. The intensity of the dynamic effects can be measured in the degrees of the difference between the velocity distributions in the 50 and 60 Hz cases.

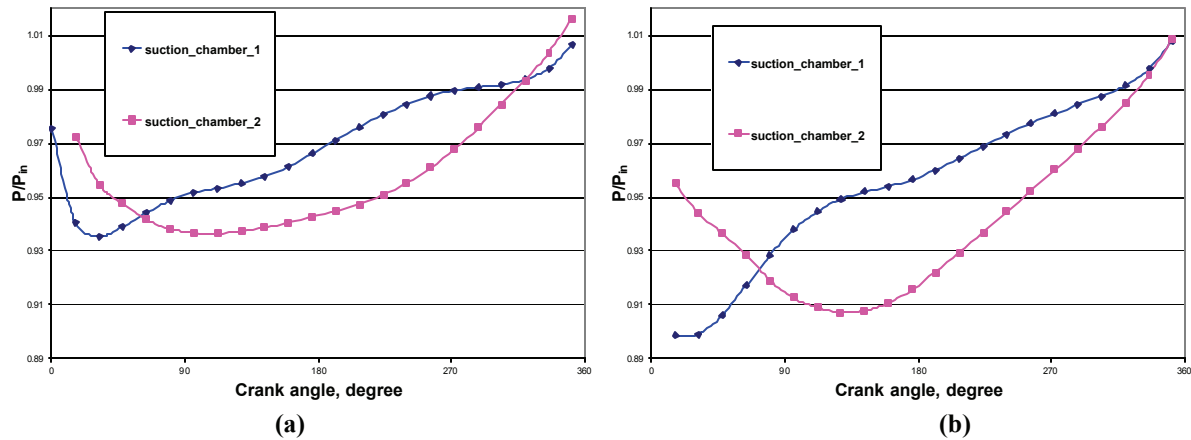


**Figure 3** Pressure distributions inside the suction chambers for the frequency of 50 Hz (a) and 60 Hz (b).

The performance difference of the scroll compressor for 50 Hz and 60 Hz power frequency can be calculated from their pressure distribution over the suction process:

$$W = \iiint_{V_1} (P_{in} - P(x, y, z)) dV(x, y, z) + \iiint_{V_2} (P_{in} - P(x, y, z)) dV(x, y, z)$$

where  $P_{in}$  is inlet pressure and  $P$  is the pressure inside the suction chambers;  $V_1$  and  $V_2$  are the volume of the suction chamber 1 and 2, respectively.

In the terms of the total compressor efficiency, the suction losses for 50 and 60 Hz are 4.09 and 4.86%, respectively. The difference of the suction losses for the 50 and 60 Hz cases is 0.77% and the compressor performs better in 50 Hz case.

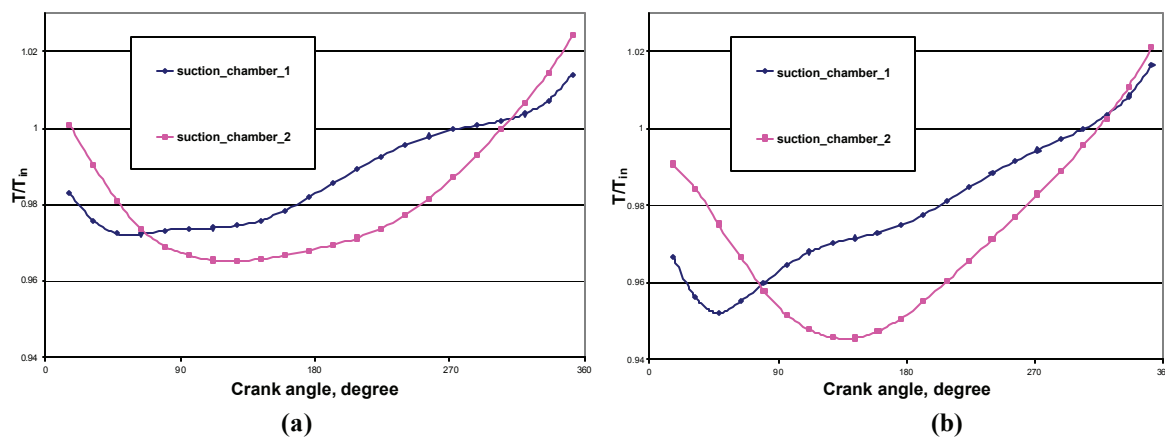
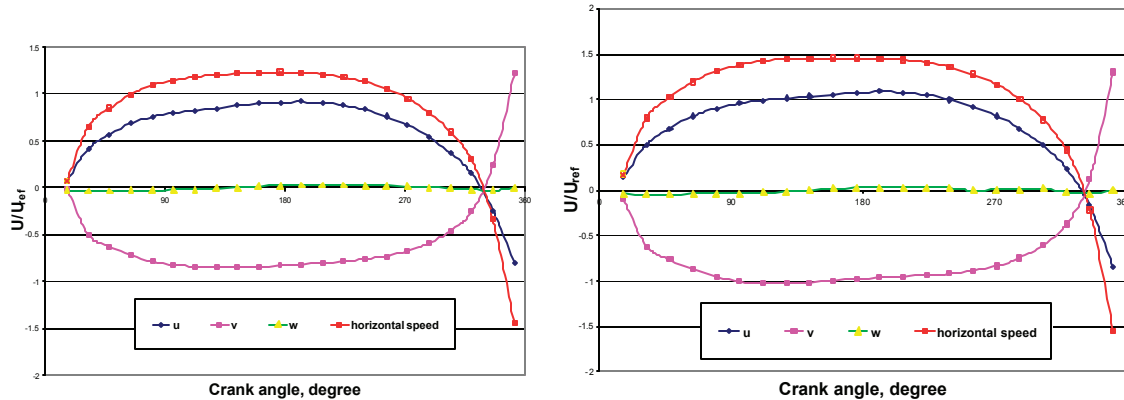


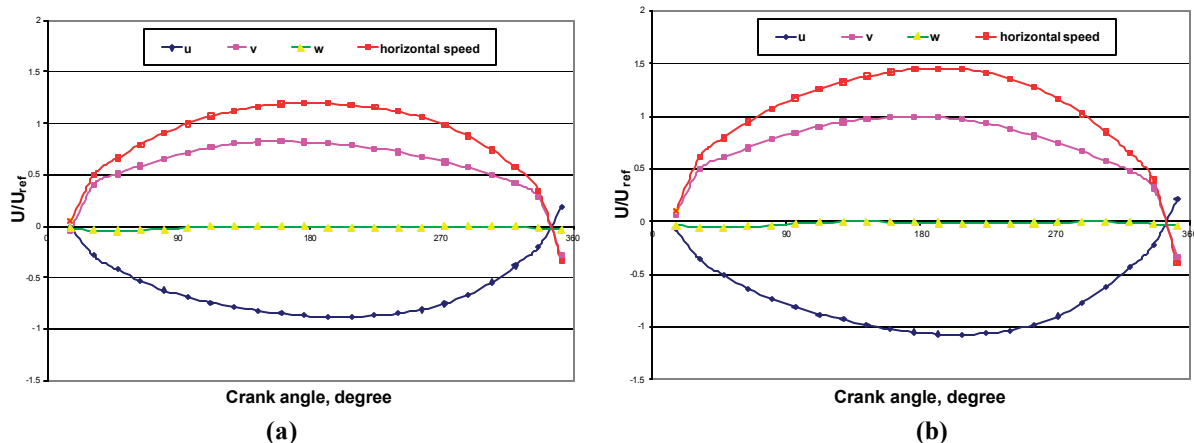
**Figure 4** Temperature distributions inside the suction chambers for the frequency of 50 Hz (a) and 60 Hz (b).

The pre-compression effect in the suction process can be observed in the suction process. Figure 2 (b) shows the volumes of both suction chambers reach their maximum values before the end of the suction process and start to compress the gas inside the suction chambers. The pressure and temperature inside the suction chamber start to surpass their values at the inlets (Figure 3 and Figure 4). The suction velocity (Figure 5) at the inlets shows the negative values that indicate the gas actually was squeezed out of the suction chambers because of the pre-

compression effect. Although the pre-compression increases the pressure values inside the suction chambers, the losses are induced because the refrigerant gas is discharged out of the suction chambers.



(a) (b)  
Figure 5 Suction velocity entering suction chamber 1 for 50 Hz (a) and 60 Hz (b).



(a) (b)  
Figure 6 Velocity entering suction chamber 2 for the frequency of 50 Hz (a) and 60 Hz (b).

### 3. COMPRESSION PROCESS

In the compression process, the comparatively independent gas pockets are compressed by the motion of the orbiting scroll. The volume of the gas pockets decreases and the pockets move along a spiral path to the center of the compressor. The time history of the volume change for these gas pockets are illustrated in Figure 7 (a). There are narrow gaps between these pockets. The refrigerant gas can leak through these gaps from upstream pockets to downstream pockets. The time histories of the leakage gaps are shown in Figure 7(b). The time period when the leakage gap opens is 20% longer in the 50 Hz case than the 60 Hz case. The volume changes faster as a function of time in the 60 Hz case. As the power frequency increases from 50 Hz to 60 Hz, Figure 7 indicates the gradient of the volume curves of the gas pockets are larger for the suction chambers on both sides. The leakage gap for the 60 Hz case opens earlier than the 50 Hz case (Figure 7(b)). However, the volume and gap variation for two sides of the compressor are identical.

The volume-averaged pressure in the gas pockets are shown in Figure 8. For generality, the pressure is plotted as a non-dimensional value using the pressure value at the compressor inlet. The pressure profiles of the two sides of the compressor are different from each other. Since the gas leaks from the upstream pockets to downstream pockets, the pressure value of the compression process for the 50 Hz case is higher than 60 Hz case for a given volume of gas pockets. Park *et al.* (2002) observed the same phenomenon.

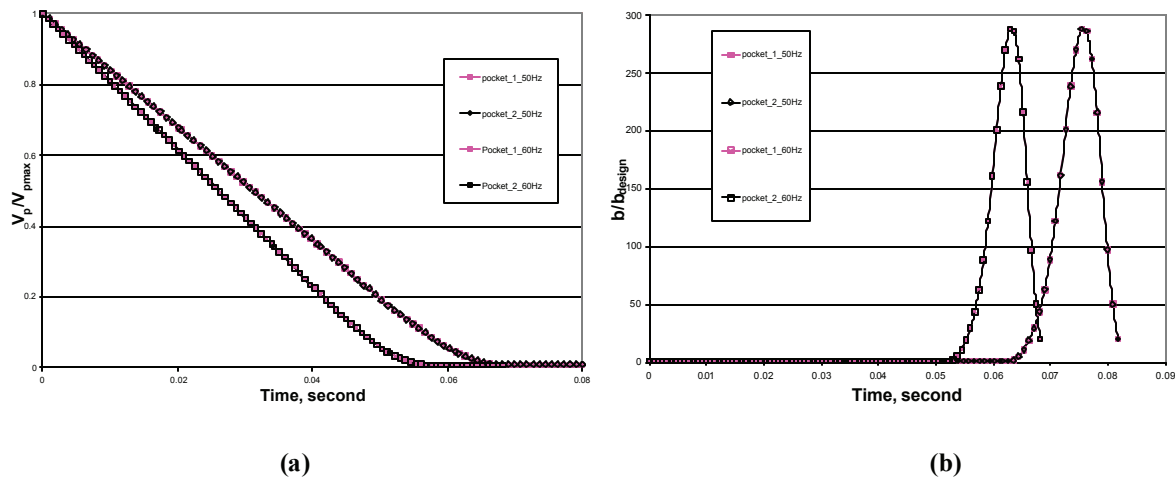


Figure 7 Volume and leakage gap for the frequency of 50 Hz (a) and 60 Hz (b).

Figure 9 shows the leakage pressure differential in the neighboring gas pockets for the 50 Hz and 60 Hz cases. In the early stage of the compression, the pressure differentials between the neighboring pockets are similar in both cases. As the gas pockets approach the center of the compressor, the difference of the pressure inside the neighboring gas pockets is slightly larger in the 60 Hz case although the absolute pressure value is higher in the 50 Hz case for the same volume of the gas pockets. There are two physical mechanisms responsible for this phenomenon. The first is the restriction of the discharge port on the through flow. In the 60 Hz case, the mass flow is 20% larger than the 50 Hz case while the size and shape of the discharge port stay the same. The second is the weaker leakage effect to equilibrate the pressure values in the two pockets connected since the time period when the leakage gap opens is shorter in the 60 Hz case.

The leakage loss is proportional to the gap opening time and pressure differential for a given flank gap. The difference of the gap opening time is 20% between the two cases. The pressure differential between the gas pockets can be affected by many design parameters: involute profile, pocket size and shape, refrigerant property, operating conditions, and designs of upstream/downstream components. For the compressor design used in the current study, the difference in the pressure differential is smaller than the difference in the leakage time that is 20% between the two cases. As a combined effect of these two mechanisms, the leakage loss is larger in the 50 Hz case which has longer opening time for the gap between the gas pockets. For this particular design the leakage loss for 50 Hz is .45 % higher compared to the 60 Hz case in the terms of the total compressor efficiency.

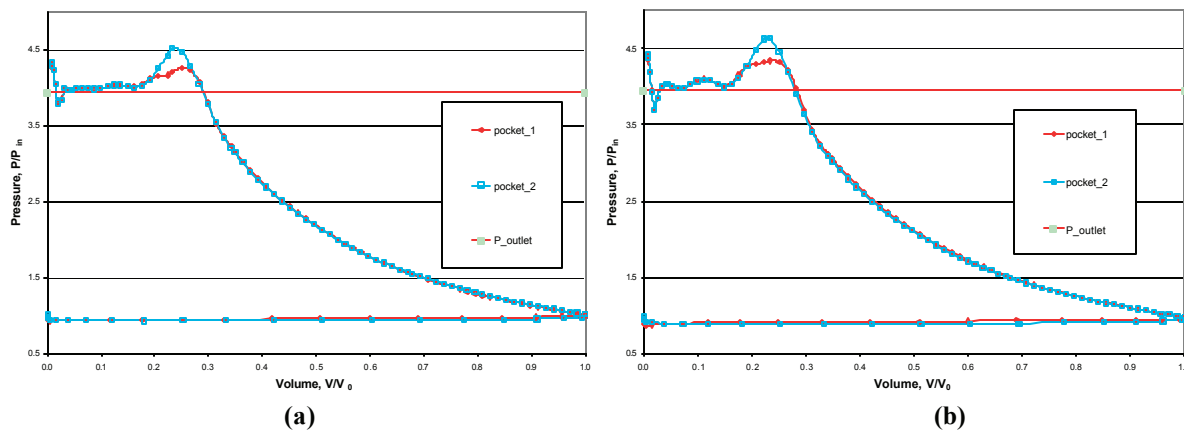


Figure 8 Compression processes of the gas pockets for the frequency of 50 Hz (a) and 60 Hz (b).

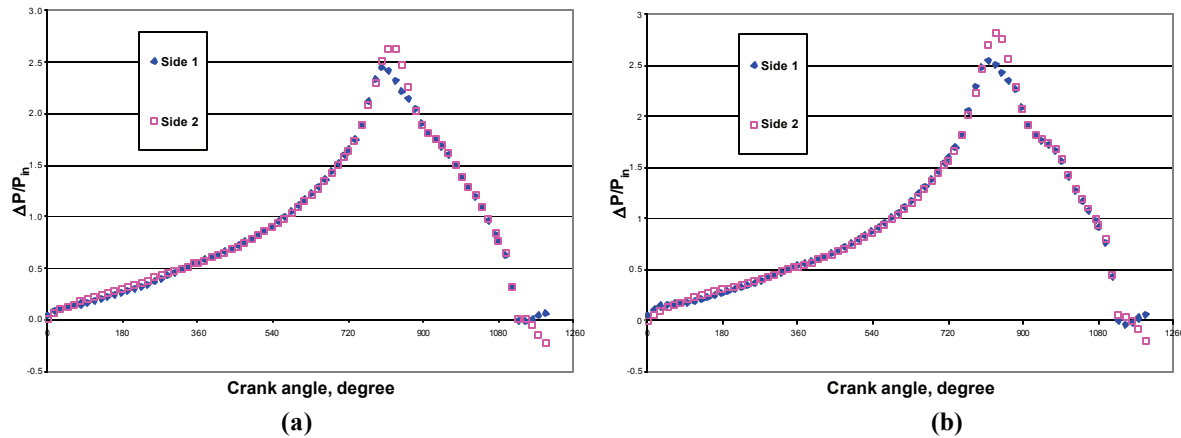


Figure 9 Leakage pressure differential for the frequency of 50 Hz (a) and 60 Hz (b).

#### 4. DISCHARGE PROCESS

In the discharge process of the compressor, the series of the gas pockets merge with each other and form a continuative gas stream again. Since the downstream components, discharge port, discharge passage, and plenum, are the same for 50 and 60 Hz cases, the larger mass flow rate in the 60 Hz case results in higher over-compression for the same scroll compressor design. Figure 8 shows the maximum pressure value is higher in the 60 Hz case than the 50 Hz case. The time period during which the pressure at the discharge port is above the compressor discharge pressure is longer in the 60 Hz case. Consequently, the work required to generate the higher pressure is larger in the 60 Hz case. For the compressor design selected for our current investigation, the over-compression loss for 60 Hz case is .66 % higher than the 50 Hz case in the terms of the total compressor efficiency.

Figure 10 displays the total and static pressure history at the discharge port for the 50 and 60Hz cases. In addition to the higher frequency, the 60 Hz case also shows a larger pressure fluctuation at the discharge port. The minimum pressure value in the 60 Hz case is lower than the 50 Hz case and the maximum pressure values are higher than the 50 Hz case. The former is caused by leakage that equilibrates the pressure in the gas pockets more in the 50 Hz case than the 60 Hz case. The later is caused by the restriction of the higher mass flow rate in the 60 Hz case.

One of the consequences of the higher mass flow rate in the 60 Hz case is the total pressure loss in the discharge process is larger in the 60 Hz case. Figure 10 shows the difference between the total and static pressures is larger in the 60 Hz case. Without a good diffusion process, the kinetic energy associated velocity is dissipated into heat and can not be used for the cooling. Therefore the discharge loss is higher in the 60 Hz case.

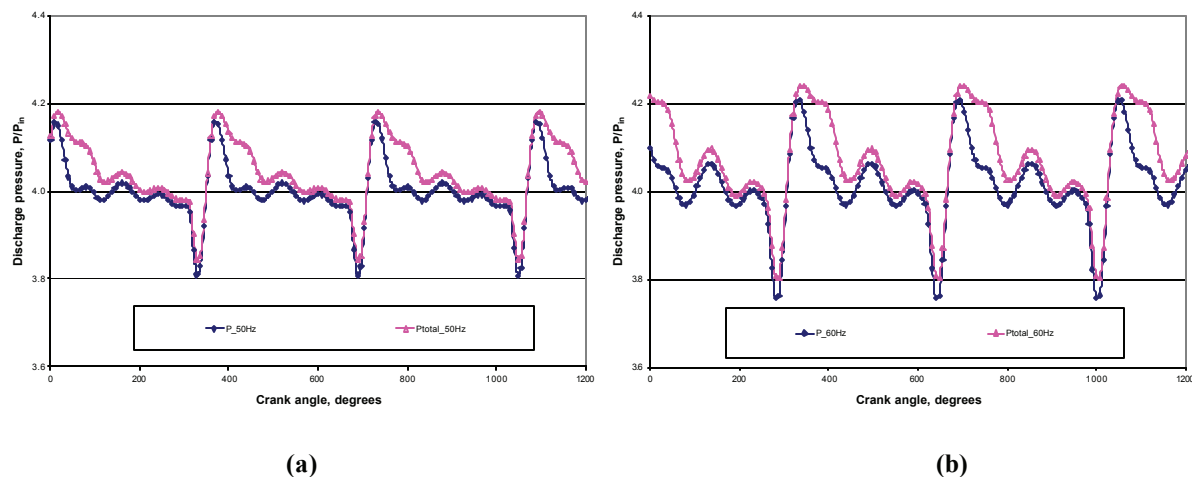


Figure 10 Static and total pressure at discharge port for the frequency of 50 Hz (a) and 60 Hz (b).



## 5. CONCLUSIONS

When a scroll compressor operates at different frequencies, the fundamental mechanisms that control the losses are different. These differences can be observed in suction, compression, and discharge processes. For the design analyzed in the current study, the frequency increase from 50 to 60 Hz increases loss in suction and discharge processes. The loss in the compression process decreases. The losses in suction, compression and discharge processes caused by the power frequency change from 50 to 60 Hz are 0.77, -0.45, and 0.66 % respectively. The total efficiency for 60 Hz case is 1% lower than the 50 Hz case.

The change rate and time-dependent profiles of the geometric features induced by the frequency change are symmetric for the gas pockets on both sides of the compressor. The physical parameters are asymmetric on two sides of the compressor even when the geometric changes are symmetric.

The characteristics of a scroll compressor working process depend on the design details of the compressor. The physical mechanisms and their relative strength are also an inherent part of the compressor design. The relative change in the performance for the frequency change depends on the particular design. It is not a general conclusion that the scroll compressors perform better in 50 Hz power frequency.

## NOMENCLATURE

$A$	area	<b>Subscripts</b>	
$b$	gap	<i>design</i>	design value
$P$	pressure	<i>in</i>	inlet
$T$	temperature	<i>out</i>	outlet
$U$	speed	$p$	pocket
$u$	x-component of velocity	$0$	initial
$V$	volume		
$v$	y-component of velocity		
$w$	z-component of velocity		
$?$	difference		

## REFERENCES

- Park, Y.C., Kim, Y., Cho, H., 2002, Thermodynamic Analysis on the Performance of a Variable Speed Scroll Compressor with Refrigerant Injection, Int. J. Refrigeration, Vol.25 (2002), pp1072-1082.
- Cho, Y., H., Lee, B. C., Lee, J. K., Development of High Efficiency Scroll Compressor for Package Air Conditioners, International Compressor Engineering Conference at Purdue, 1996, pp323-328.
- Hirano, T., Matsumura, N., Takeda, K., Development of High Efficiency Scroll Compressor for Air Conditions, International Compressor Engineering Conference at Purdue, 1988, pp65-74.
- Cui, M., 2003, Numerical Study of Unsteady Flows in a Scroll Compressor, Proceedings of the International Conference on Compressors and their Systems, London, 2003, pp2-10.
- Cui, M., Sauls, J., 2006, Investigation of Suction Process of Scroll Compressors, International Compressor Engineering Conference at Purdue, C110, 2006.

## ACKNOWLEDGEMENT

The authors would like to thank The TRANE Company for the permission to publish this paper.